Statistical Uncertainty of PM-measurements Based on Laser-Scattering Sensors

Bernd Laquai, 14.11.2017

Introduction

Today's PM-measurements are often performed with laser scattering instruments or sensors, that use the light scattered from particles to determine particle size as well as particle count rates. From the count rates number and mass concentration are derived.

Actually, such an instrument that counts particles according to their size has to be perceived a set of N sub-instruments working in parallel, each performing the same calculation for the number of particles counted in one of the N bins but for different size d. For the total result to be accurate, each individual bin calculation has to be accurate. From the perspective of measurement uncertainty, each of the N sub-instruments contributes with its individual size dependent uncertainty.

Since the actual measurement in each bin is based on counting particles that arrive at random points in time, we are faced with the fact that the measurement value – the count rate – has to be determined from a limited sample set with respective statistical uncertainty. Since the uncertainty depends on the sample size acquired over time, it will be determined by the the measurement time. In other words, the faster an instrument can gather particles of a given size, the faster it can provide measurement results with a given accuracy. In contrast to a professional PM laser scattering instrument with a sample volume flow of several l/min, a low-cost PM sensor typically counts particles from a small volume flow of about 100ml/min and less. This means, accurate measurements values are not achieved before enough air volume has passed through the sensor device which may take hours. As a consequence, rapid changes in PM mass concentration can no longer be distinguished from statistical noise and therefore can't be resolved accordingly. When such a low-cost sensor is deployed for mobile measurements, the spatial resolution is also limited when a certain velocity is given.

The above considerations indicate that it is imperative to know the uncertainties as a result of statistical fluctuations when count rates are determined from randomly arriving particles in different size bins, in order to calculate number or mass concentration. The PM mass concentration in each bin has to be provided with the respective uncertainty and the propagation of the bin specific uncertainties into PM-values has to be considered. When the size bins are summed up to a value such as PM10, the individual uncertainty contributions from each bin have to be taken into account accordingly to finally determine the uncertainty of the PM10 value or to determine the time required for measuring PM10 with a given measurement uncertainty. Due to the smaller volume flow the determination of statistical measurement uncertainty is imperative, particularly for low-cost laser scattering PM-sensors

Uncertainties of PM measurements – theoretical considerations

In order to investigate the uncertainty of PM measurements it is helpful to have a closer look to other scientific disciplines, where counted measurements already have a certain history and the relationships are already well understood and analyzed in depth. One scientific discipline where counted measurements had been used since its beginning is nuclear science. The most well-known

instrument for quantitative measurements of radioactivity is the Geiger-Muller counter that is still commercially available and frequently used today. When such an instrument is placed on a sample of 1kg of potassium fertilizer for example, a significant increase of the famous clicking sound can be observed when the instrument used is also equipped with an audio output. The natural occurring potassium that is contained in high concentration in a fertilizer, always contains about 0.012% of the radioactive K-40 isotope. The K-40 isotope decays to about 90% into Ca-40 which is stable, emitting an electron (beta particle) and a gamma quantum (radiation). Both, the electron and the gamma radiation causes an ionization event in the GM-tube, audible as a click in a GM-counter. According to /1/ the measurable impulse rate is about 18.9 counts/min (determined from a time interval of 30min) when a KCl containing fertilizer (e.g. Kornkali ™) is arranged as a 15mm thick layer below the GM-counter.

It is well known, that the number of clicks observed during a given measurement time follow the Poisson distribution. Additionally, it can be observed that the time between particles is distributed according to a negative exponential distribution with a time constant t_{ave}, which is the expected value of this distribution. Both is the consequence of the fact, that the probability of the decay of a single atom is independent of its age. More generically spoken, the nuclear decay is a memoryless random process. A key property of the Poisson distribution is the fact that its standard deviation is the square root of its mean. Therefore, when counting N clicks, the 1σ statistical uncertainty is $\pm\sqrt{N}$. For N > 30 the Poisson distribution can be approximated by a Gaussian distribution with $\mu=N$ and $\sigma=\sqrt{N}$.

In contrary, when observing the failures of technical systems or the mortality of biological systems, these random processes are not ideally memoryless but depend on age. A higher infant mortality for example implies that failure or mortality will not follow the Poisson statistics. However, since the arrival of particles does not depend on the arrival of previous particles or the age of particles, the arrival of particles in a measurement chamber is supposed to be a memoryless process. Therefore, the detection of laser scattering pulses will follow the Poisson statistics in a similar way as when counting alpha- or beta-particles or gamma-quanta with a Geiger-Muller counter.

Professional PM-measurement equipment typically uses a sample volume stream of about 1-5 liter/min to determine the number concentration of particles. This number concentration is then converted into particle mass, mostly using a particle model based on perfectly spherical particles and a density of the bulk material of $1g/cm^3$. Furthermore, such an instrument sorts the particles into typically 16 particle size bins according to the intensity of the scattering light pulses.

From the simple theory of ideally spherical particles it becomes obvious that in presence of a mass concentration of e.g. $10\mu g/m^3$ and assuming only particles of a10µm size, a theoretical average of 19.1 particles can be found in one liter of sampled air ($\rho = 1g/cm^3$). If we could count these particles with a counting efficiency of 100%, the number concentration per liter sampled with an air flow of 1l/min in 1 minute will be measured to be $c_N = 19.1 \pm \sqrt{19.1}$ [1/l] = 19.1 ± 4.37 [1/l] according to the Poisson theory. Therefore, the uncertainty in the number concentration in this case will be 23%.

In general, we can state, based on the Poisson statistics that the rate of observed particles in an air stream is:

$$r' = N'/T = (N \pm \sqrt{N})/T = r * (1 \pm 1/\sqrt{N}) \qquad (1)$$

when N' is the observed number of particles in an air sample of given measurement time T, and when N and r are the mean values observed in an infinitely long time interval.

When V_F is the volume flow, we can determine the mean value of the number concentration c_N:

$c_N = N/(V_F * T)$ (2)

Therefore, the uncertainty of the number concentration measurement can be derived in a similar way:

$c_N' = c_N * (1 \pm 1/\sqrt{N})$ (3)

Since for the mean values we also have the relationship:

$\sqrt{N} = (T/t_{ave})^{1/2}$ (4)

we can specify the sample based number concentration in terms of measurement time T and mean time between particles t_{ave}:

$c_{N,1\sigma}' = c_N * (1 \pm (t_{ave}/T)^{1/2})$ (5)

This number concentration c_N' estimated from a sample set is based on 1σ of the Poisson distribution.

For a 2σ uncertainty we get:

$c_{N,2\sigma}' = c_N * (1 \pm 2*(t_{ave}/T)^{1/2})$ (6)

For N>30 we can assume a Gaussian behavior of the Poisson distribution, therefore we can assign a 68% confidence interval to the 1σ estimation and a 95% confidence interval to the 2σ estimation of c_N'.

Since the total volume V used for sampling is:

$V = V_F * t_{ave}$ (7)

and N particles are contained in this volume in average, the mean time t_{ave} between particles is given by:

$t_{ave} = 1 / (N * V_F)$ (8)

For ideally spherical particles, the relationship between mass and number concentration is:

$c_M = c_N * \pi/6 * \rho * d^3$ (9)

Therefore, the sample based mass concentration for the particles can be derived with its uncertainty from the sample based number concentration:

$c_M' = c_N' * \pi/6 * \rho * d^3 = c_M * (1 \pm (t_{ave}/T)^{1/2})$ (10)

This finally means, that the number concentration c_N' as well as the mass concentration c_M', when determined from particles that arrive at the counting sensor in a given mean time show an uncertainty that depends on the squared ratio $(t_{ave}/T)^{1/2}$ between average time between particles t_{ave} and measurement time T. The less time elapses between the arriving particles in average, the more particles will make up the sample set from which the concentration will be determined and the less is the uncertainty. This result is not really surprising since the squared ratio just expresses the Poisson characteristic of the particle arrival process of N particles translated into the time domain.

The following graphs show the overlaid results of Monte-Carlo simulations on the determination of the mass concentration along an increasing measurement time. For each of the 500 measurement runs overlaid in one graph, the neg.-ex. distributed time of 4000 laser scattering events was simulated. The overlays were generated for a volume flow of 1.2l/min (e.g. Grimm 1.108) and

0.1l/min (e.g. a low-cost sensor) for the 10um size bin. The overlay for 1.2l/min is shown for a mass concentration of 10 µg/m^3 only, whereas for the 0.1l/min volume flow the overlay shown for 10 and 100µg/m^3. The red lines indicate the theoretical uncertainty calculated from the 2σ uncertainty according to (10).

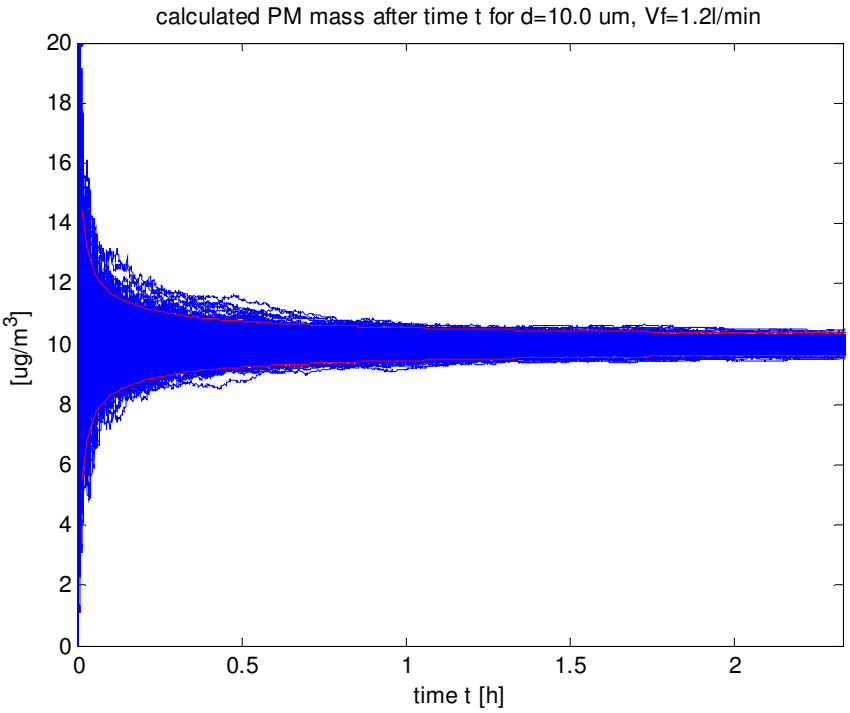

Fig. 1a: Monte-Carlo simulation of the converging mass calculation versus measurement time for a flow rate of 1.2l/min and an expected mass value of 10µg/m^3 (blue: overlay of 500 measurement executions, red: theoretical 2σ uncertainty)

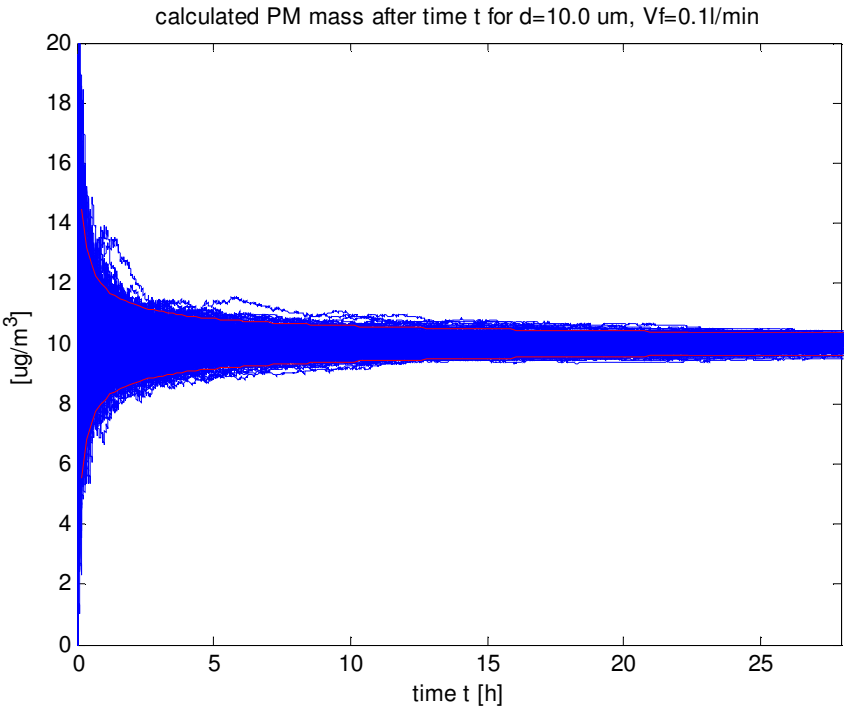

Fig. 1b: Monte-Carlo simulation of the converging mass calculation versus measurement time for a flow rate of 0.1/min and an expected mass value of 10µg/m^3 (blue: overlay of 500 measurement executions, red: theoretical 2σ uncertainty)

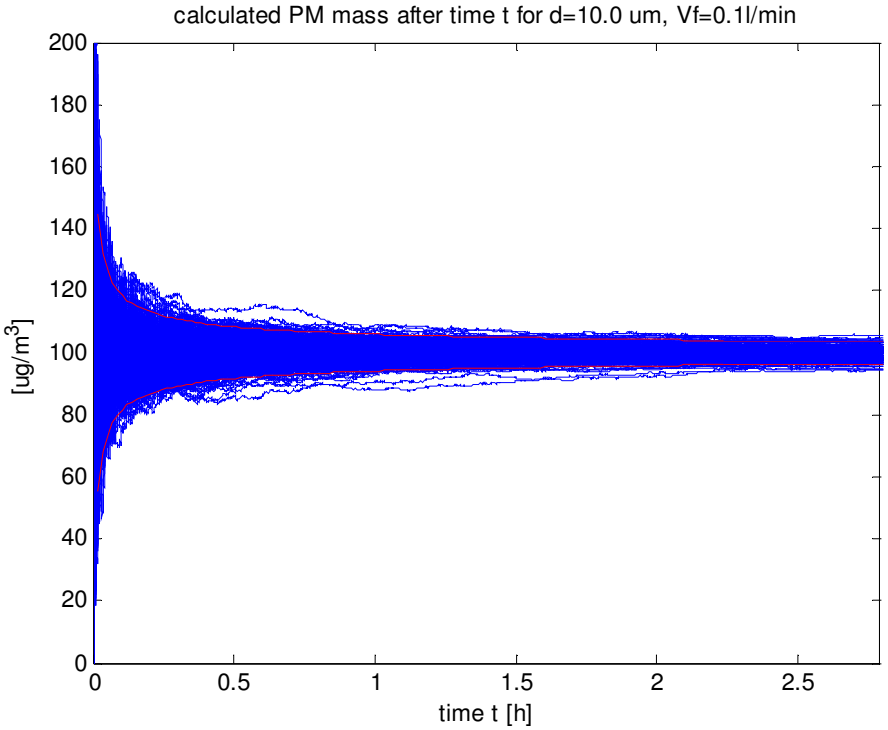

Fig. 1c: Monte-Carlo simulation of the converging mass calculation versus measurement time for a flow rate of 0.1l/min and an expected mass value of 100µg/m^3 (blue: overlay of 500 measurement executions, red: theoretical 2σ uncertainty)

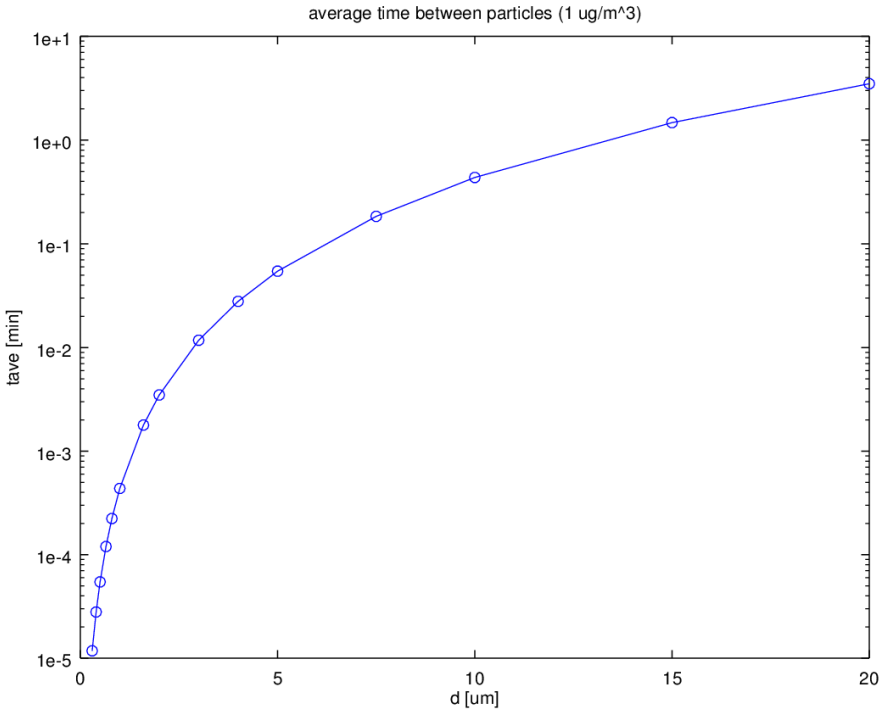

Fig. 2: Average time t_{ave} between 10µm particles for a volume flow of 1.2l/min and a mass concentration of 1 µg/m^3, the dots mark the bin sizes of the Grimm 1.108 aerosol spectrometer

	Vf=1.2l/min	
d [µm]	tave	time unit
0.3	7.07E-04	s
0.4	1.68E-03	s
0.5	3.27E-03	s
0.65	7.19E-03	s
0.8	1.34E-02	s
1	2.62E-02	s
1.6	1.07E-01	s
2	2.09E-01	s
3	7.07E-01	s
4	1.68E+00	s
5	3.27E+00	s
7.5	0.18	min
10	0.44	min
15	1.47	min
20	3.49	min

	Vf=0.22l/min	
d [µm]	tave	time unit
0.46	1.39E-02	s
0.66	4.11E-02	s
0.89	1.01E-01	s
1.15	2.17E-01	s
1.45	4.35E-01	s
1.85	9.04E-01	s
2.55	2.37E+00	s
3.5	6.12E+00	s
4.5	0.22	min
5.75	0.45	min
7.25	0.91	min
9	1.74	min
11	3.17	min
13	5.23	min
15	8.03	min

Table 1: Average time t_{ave} between 10µm particles for a volume flow of 1.2l/min (Grimm 1.108) and a volume flow of 0.22l/min (Alphasense OPC-N2), assuming a mass concentration of 1 µg/m^3

Table 1 shows the values of the time between the particle arrival for 1ug/m^3 of particle mass in the 10µm size bin for a volume flow of 1.2l/min of the Grimm 1.108 instrument and the Alphasense OPC-N2 low-cost sensor (0.22l/min). As it can be seen, the 10µm (Grimm 1.108) and the respective 9um bin (Alphasense OPC-N2) show significantly different values for t_{ave}. Whereas the sample flow based t_{ave} of the Grimm 1.108 is 0.44min the corresponding value of the Alphasense is 1.74min. In order to achieve a 1σ uncertainty of less than 10%, the expression $(t_{ave}/T)^{½}$ needs to be 0.1, this means a measurement time T is required that is 100 times larger than t_{ave}. In the case of the Grimm 1.108 this will be 44 minutes, in case of the Alphasense this will be 2.9 hours. When the mass concentration in the 10µm size bin increases, the time t_{ave} decreases inversely proportional. E.g. for 10µg/m^3 the average time between particles t_{ave} would be 4.4min for the Grimm and for the Alphasense it would be 0.29h.

Some of the professional instruments, but also low-cost sensors like the Alphasense OPC-N2 provide c_N' or c_M' particle concentration data for each bin (sometimes called differential count dN or differential mass dM). These data allow the determination of t_{ave} and thus the uncertainty of the respective sample counts or sample mass in each bin directly from measurement. The advantage of using t_{ave} extracted from measurements is the fact that the above theoretical determination assumes a 100% count efficiency. In reality the instrument does not see all of the particles contained in the sample volume stream. So a value for t_{ave} estimated from the theoretical amount of particles contained in a volume at a given mass concentration is just the best case. A more realistic value of the time between particles can be extracted from an instrument measurement when sorting timestamps of non-null counts along increasing time and then calculating the difference between the timestamps.

To finally estimate the statistical uncertainty of a PM10 calculation, we have to take into account that PM10 is actually the forming of a sum along the measured differential mass concentrations c_{Mi}' in different size bins up to a certain size. Actually, according to definition, an additional weighting has to be done reflecting a filtering characteristic, such that 50% of the 10µm particles are filtered out. For this estimate however, we just assume that the sum of the bins contains the 10µm bin as the largest bin being relevant for PM10:

$$PM10 = c_{M1}' + c_{M2}' + \ldots + c_{Mi}' + c_{Mk}' \qquad (11)$$

where k is the index of the 10um bin. Since this is a plain sum, we can state that also all uncertainties from the individual bins sum up to the gross uncertainty of PM10. As the largest particles have the largest value for t_{ave}, the PM10 uncertainty is dominated by the uncertainty of the 10µm bin, provided an equally distributed mass distribution. However, since we can assume that the arrivals of particles in the measurement chamber are independent of size and are not correlated between each other, we can formulate the calculation of PM10 including the statistical uncertainties from the individual size bins as follows:

$$PM10_{1\sigma}' = c_{M1} * (1\pm (t_{ave,1}/T)^{½}) + c_{M2} * (1\pm (t_{ave,2}/T)^{½}) + \ldots c_{Mi} * (1\pm (t_{ave,i}/T)^{½}) + \ldots + c_{Mk} * (1\pm (t_{ave,k}/T)^{½}) \qquad (12)$$

However, summing up the individual uncertainties in terms of a maximum error would be a pretty conservative estimate of the total uncertainty. Based on the Gaussian error propagation theory, a root mean square error sum would be much more appropriate. Applying the Gaussian error theory to the estimate of PM10 uncertainty, we finally arrive at an expression that seems to be well applicable to most of the cases:

$$PM10_{1\sigma}' = PM10 + (1/T*(c_{M1}^{\ 2} * t_{ave,1} + c_{M2}^{\ 2} * t_{ave,2} + ... c_{Mi}^{\ 2} * t_{ave,i} + ... + c_{Mk}^{\ 2} * t_{ave,k}))^{½} \quad (13)$$

In this expression, the c_{Mi} are the mass concentrations in the individual size bins i up to the bin k, the largest bin relevant for PM10. The values $t_{ave,i}$ are the respective times between particle arrivals, either calculated from the theory of spherical particles, neglecting the counting efficiency, or extracted from the measurement supposing a constant mass concentration in average.

Since the spherical particle theory tells us, that $t_{ave,i}$ drops with the power of 3, similar as the particle size for a constant particle mass, the PM10 uncertainty estimate will be dominated by the contributions from the large size bins. When a significant amount of mass is concentrated in the 10µm size bin, it therefore will be sufficient to estimate the uncertainty or the required measurement time from c_{Mk} and $t_{ave,k}$, with k being the index of the 10um size bin.

In general, for a value like PM2.5, a similar approach can be used as for PM10. However, since the average times between particles are dramatically smaller, the sample sizes are huge und the statistical uncertainty will only be a problem in cases when very small mass concentrations have to be measured.

Uncertainties of PM measurements – practical measurement results

As an instrument example, the Grimm 1.108 aerosol spectrometer provides a C-file for number concentrations and a dM-file for mass concentrations along with each measurement interval showing per bin results for each individual size bin. Data for all size bins are available for each measurement interval that can be set in a configuration menu.

Fig. 4a shows an excerpt of a C-file for the PM-measurement shown in fig. 3 which was taken at a high traffic road in Stuttgart downtown on a sunny September afternoon during rush hour. Fig. 5b shows an excerpt of the respective dM-file. PM10 as reported by the instrument can alternatively be calculated by summing up the per bin data in each line of the dM-File and applying the filter separation characteristic for PM10 as given in the appendix of the user manual. The given separation characteristic filters the fraction of particles < 10µm with a 50% crossover at 10µm. A similar result is achieved when the C-data are weighted according the relationship (9) to obtain the differential mass dM directly from dN.

When carefully looking at the dN data it can be seen, that in the higher bins, the dN counts often are either null or are multiples of 10 (1.6µm bit – 20µm bin) or multiples of 50 for the smaller sizes. This behavior can be seen in a very pronounced way, when the instrument had measured a low PM mass concentration and each bin is sorted individually for increasing values. After sorting, the first non-null number is the smallest count assigned during a measurement. Actually, it means that the instrument assigns 10 counts in the C-file (dN-data) for each physically registered light scattering pulse that was attributed to the 10µm bin from the pulse height analyzer. In the same way, it can be seen that the instrument assigns a minimum mass concentration value of 26.59µg/m^3 for each physically registered light scattering pulse that was attributed to the 10µm bin. These values reflect the

counting efficiency of the instrument and respectively the mass assignment to a single physically registered scattering pulse.

This functionality can also be visualized with the instrument software when the temporal display of the 10µm bin (fig. 5a) or the 20µm bin (fig. 5b) is selected.

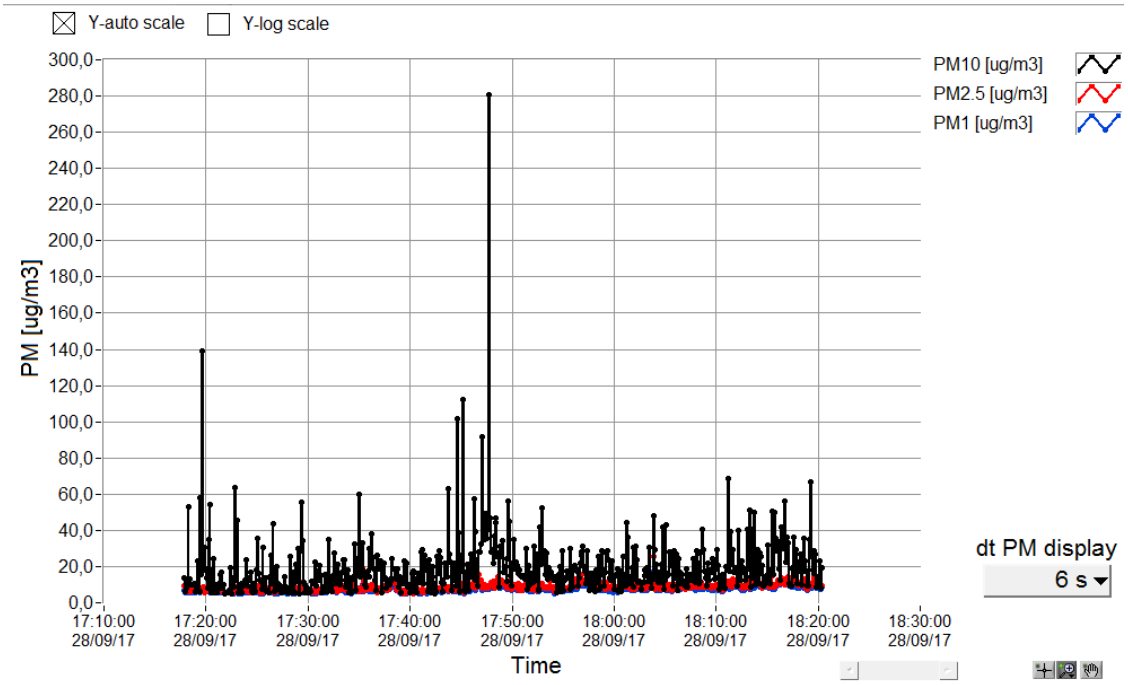

Fig. 3: PM-values displayed versus time (Grimm 1.108 Software)

counts [1/l] | mass [ug/m3] | log

date & time	0,30 um	0,40 um	0,50 um	0,65 um	0,80 um	1,00 um	1,60 um	2,00 um	3,00 um	4,00 um	5,00 um	7,50 um	10,00 um	15,00 um	20,00 um
9.2017 17:17:51	25760,0	6760,0	1750,0	200,0	100,0	50,0	90,0	150,0	0,0	0,0	10,0	0,0	0,0	0,0	0,0
9.2017 17:17:57	21680,0	5550,0	1150,0	150,0	0,0	100,0	0,0	0,0	0,0	0,0	0,0	0,0	0,0	0,0	0,0
9.2017 17:18:03	22890,0	5400,0	1000,0	100,0	100,0	100,0	60,0	30,0	10,0	0,0	0,0	0,0	0,0	0,0	0,0
9.2017 17:18:09	21680,0	4700,0	1350,0	200,0	0,0	0,0	120,0	160,0	20,0	0,0	0,0	0,0	0,0	0,0	0,0
9.2017 17:18:15	22180,0	6010,0	950,0	250,0	100,0	0,0	0,0	0,0	30,0	0,0	10,0	30,0	20,0	10,0	0,0
9.2017 17:18:21	21180,0	5000,0	950,0	50,0	0,0	150,0	0,0	40,0	0,0	0,0	10,0	0,0	0,0	0,0	0,0
9.2017 17:18:27	20980,0	5250,0	700,0	100,0	100,0	150,0	30,0	80,0	20,0	10,0	10,0	0,0	0,0	0,0	0,0
9.2017 17:18:33	20930,0	5500,0	950,0	250,0	100,0	0,0	0,0	20,0	20,0	0,0	10,0	0,0	0,0	0,0	0,0
9.2017 17:18:39	22330,0	5350,0	750,0	50,0	50,0	100,0	50,0	40,0	0,0	0,0	10,0	0,0	0,0	0,0	0,0
9.2017 17:18:45	20420,0	5410,0	1600,0	50,0	0,0	200,0	170,0	130,0	0,0	0,0	0,0	0,0	0,0	0,0	0,0
9.2017 17:18:51	22180,0	5910,0	950,0	100,0	50,0	50,0	0,0	50,0	40,0	10,0	0,0	0,0	0,0	0,0	0,0
9.2017 17:18:57	21820,0	4550,0	600,0	200,0	50,0	0,0	0,0	0,0	0,0	0,0	0,0	0,0	0,0	0,0	0,0
9.2017 17:19:03	21880,0	4950,0	950,0	350,0	50,0	0,0	0,0	10,0	30,0	0,0	10,0	0,0	0,0	0,0	0,0
9.2017 17:19:09	23340,0	4300,0	1350,0	150,0	50,0	0,0	0,0	0,0	10,0	10,0	10,0	20,0	0,0	0,0	0,0
9.2017 17:19:15	22530,0	4900,0	1100,0	200,0	50,0	50,0	0,0	0,0	0,0	0,0	0,0	0,0	0,0	0,0	0,0
9.2017 17:19:21	22630,0	4950,0	950,0	100,0	50,0	0,0	0,0	0,0	0,0	0,0	0,0	0,0	0,0	0,0	0,0
9.2017 17:19:27	21280,0	5000,0	800,0	200,0	50,0	200,0	0,0	0,0	0,0	0,0	50,0	10,0	30,0	0,0	10,0
9.2017 17:19:33	25800,0	5360,0	2000,0	250,0	50,0	0,0	40,0	50,0	30,0	20,0	10,0	0,0	0,0	0,0	0,0
9.2017 17:19:39	25260,0	6360,0	1400,0	200,0	250,0	100,0	0,0	0,0	0,0	0,0	0,0	0,0	110,0	40,0	0,0
9.2017 17:19:45	24040,0	5610,0	1200,0	200,0	0,0	150,0	70,0	70,0	40,0	10,0	0,0	10,0	0,0	0,0	0,0
9.2017 17:19:51	20170,0	4650,0	950,0	200,0	0,0	50,0	0,0	0,0	10,0	50,0	30,0	0,0	10,0	0,0	0,0
9.2017 17:19:57	23440,0	5050,0	1000,0	450,0	0,0	150,0	0,0	0,0	10,0	20,0	10,0	10,0	0,0	0,0	0,0
9.2017 17:20:03	23290,0	4600,0	1100,0	250,0	100,0	150,0	90,0	20,0	20,0	10,0	0,0	0,0	0,0	10,0	0,0
9.2017 17:20:09	24540,0	4400,0	1000,0	150,0	0,0	0,0	10,0	30,0	10,0	0,0	0,0	0,0	0,0	0,0	0,0
9.2017 17:20:15	22030,0	5310,0	1300,0	450,0	150,0	0,0	0,0	60,0	40,0	60,0	30,0	0,0	10,0	0,0	0,0
9.2017 17:20:21	21830,0	5260,0	1150,0	200,0	100,0	150,0	150,0	210,0	30,0	30,0	40,0	20,0	10,0	10,0	0,0
9.2017 17:20:27	22230,0	5150,0	900,0	100,0	0,0	50,0	0,0	0,0	30,0	10,0	10,0	0,0	0,0	0,0	0,0
9.2017 17:20:33	21980,0	6760,0	950,0	100,0	0,0	50,0	0,0	0,0	0,0	0,0	0,0	0,0	0,0	0,0	0,0
9.2017 17:20:39	21380,0	4900,0	1000,0	100,0	50,0	0,0	100,0	70,0	0,0	10,0	10,0	10,0	0,0	0,0	0,0
9.2017 17:20:45	21080,0	5300,0	1300,0	100,0	50,0	100,0	40,0	70,0	10,0	0,0	20,0	0,0	10,0	0,0	0,0
9.2017 17:20:51	20510,0	3450,0	1150,0	0,0	50,0	0,0	0,0	0,0	0,0	0,0	0,0	0,0	0,0	0,0	0,0
9.2017 17:20:57	21570,0	4250,0	950,0	150,0	100,0	100,0	10,0	30,0	0,0	0,0	10,0	0,0	0,0	0,0	0,0
9.2017 17:21:03	20580,0	5600,0	1050,0	200,0	50,0	50,0	0,0	0,0	0,0	0,0	0,0	0,0	0,0	0,0	0,0

Fig 4a: Differential number concentrations dN per size bin (Grimm 1.108 Software)

mass distribution (differential) [ug/m3]

0,65 um	0,80 um	1,00 um	1,60 um	2,00 um	3,00 um	4,00 um	5,00 um	7,50 um	10,00 um	15,00 um	20,00 um
0,10	0,10	0,15	0,71	3,19	0,00	0,00	3,32	0,00	0,00	0,00	0,00
0,08	0,00	0,30	0,00	0,00	0,00	0,00	0,00	0,00	0,00	0,00	0,00
0,05	0,10	0,30	0,48	0,64	0,58	0,00	0,00	0,00	0,00	0,00	0,00
0,10	0,00	0,00	0,95	3,40	1,17	0,00	0,00	0,00	0,00	0,00	0,00
0,13	0,10	0,00	0,00	0,00	1,75	0,00	3,32	27,36	53,18	72,96	0,00
0,03	0,00	0,45	0,00	0,85	0,00	0,00	3,32	0,00	0,00	0,00	0,00
0,05	0,10	0,45	0,24	1,70	1,17	1,24	3,32	0,00	0,00	0,00	0,00
0,13	0,10	0,00	0,00	0,43	1,17	0,00	3,32	0,00	0,00	0,00	0,00
0,03	0,05	0,30	0,40	0,85	0,00	0,00	3,32	0,00	0,00	0,00	0,00
0,03	0,00	0,60	1,35	2,77	0,00	0,00	0,00	0,00	0,00	0,00	0,00
0,05	0,05	0,15	0,00	1,06	2,33	1,24	0,00	0,00	0,00	0,00	0,00
0,10	0,05	0,00	0,00	0,00	0,00	0,00	0,00	0,00	0,00	0,00	0,00
0,18	0,05	0,00	0,00	0,21	1,75	0,00	3,32	0,00	0,00	0,00	0,00
0,08	0,05	0,00	0,00	0,00	0,58	1,24	3,32	18,24	0,00	0,00	0,00
0,10	0,05	0,15	0,00	0,00	0,00	0,00	0,00	0,00	0,00	0,00	0,00
0,05	0,05	0,00	0,00	0,00	0,00	0,00	0,00	0,00	0,00	0,00	0,00
0,10	0,05	0,60	0,00	0,00	0,00	0,00	16,62	9,12	79,77	0,00	212,71
0,13	0,05	0,00	0,32	1,06	1,75	2,48	3,32	0,00	0,00	0,00	0,00
0,10	0,25	0,30	0,00	0,00	0,00	0,00	0,00	0,00	292,48	291,84	0,00
0,10	0,00	0,45	0,56	1,49	2,33	1,24	0,00	9,12	0,00	0,00	0,00
0,10	0,00	0,15	0,00	0,00	0,58	6,20	9,97	0,00	26,59	0,00	0,00
0,23	0,00	0,45	0,00	0,00	0,58	2,48	3,32	9,12	0,00	0,00	0,00
0,13	0,10	0,45	0,71	0,43	1,17	1,24	0,00	0,00	0,00	72,96	0,00
0,08	0,00	0,00	0,08	0,64	0,58	0,00	0,00	0,00	0,00	0,00	0,00
0,23	0,15	0,00	0,00	1,28	2,33	7,44	9,97	0,00	26,59	0,00	0,00
0,10	0,10	0,45	1,19	4,47	1,75	3,72	13,29	18,24	26,59	72,96	0,00
0,05	0,00	0,15	0,00	0,00	1,75	1,24	3,32	0,00	0,00	0,00	0,00
0,05	0,00	0,15	0,00	0,00	0,00	0,00	0,00	0,00	0,00	0,00	0,00
0,05	0,05	0,00	0,79	1,49	0,00	1,24	3,32	9,12	0,00	0,00	0,00
0,05	0,05	0,30	0,32	1,49	0,58	0,00	6,65	0,00	26,59	0,00	0,00
0,00	0,05	0,00	0,00	0,00	0,00	0,00	0,00	0,00	0,00	0,00	0,00

Fig. 4b: Differential mass concentrations dM per size bin (Grimm 1.108 Software)

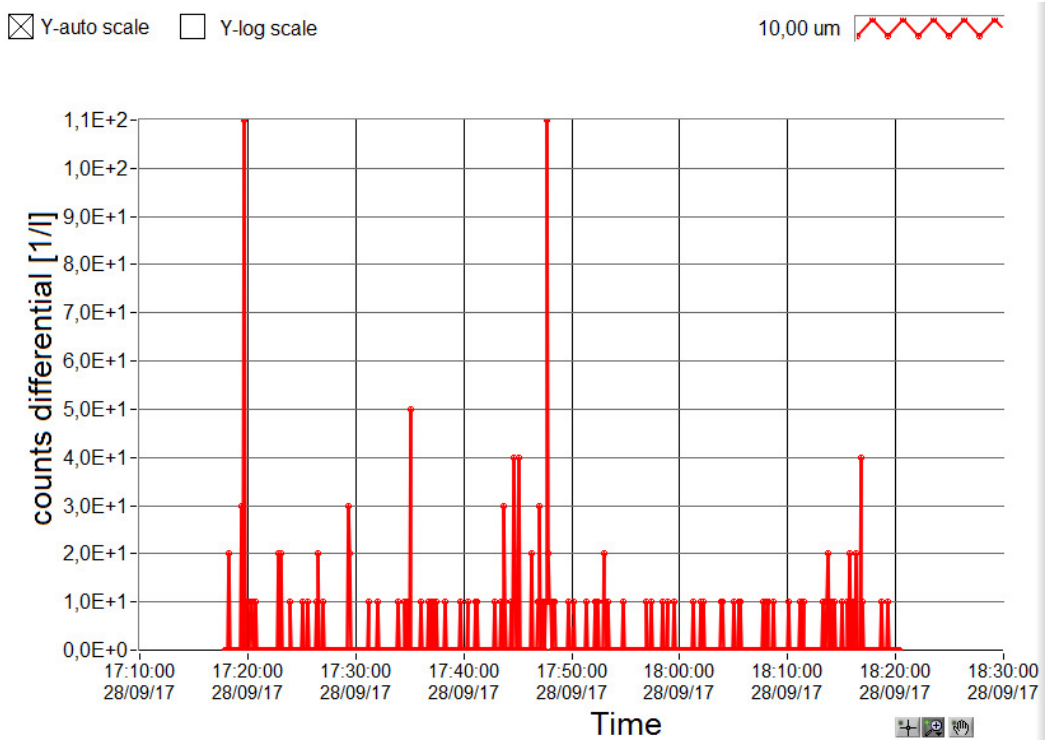

Fig. 5a: Display of the counts in the 10µm size bin versus time (Grimm 1.108 software)

Observing the signal trace of the number concentration in fig. 5a showing the 10µm bin, it becomes obvious, that in the selected measurement interval of 6s, many values report zero, many 10, a few 20, another few 30 a single one 50 and two times 110. A value of 20 occurs when two physical pulses fall in a 6s interval. Fig. 5b shows the signal trace of the 20um bin. Here, the pulses with non-null traces occur even more sparsely. From this graph the random time between particles t_{ave} quickly becomes apparent. When the mass contribution in a size bin is not high (in clean air) and therefore the particles do not occur frequently, in many cases only one single light scattering event occurs in a 6s minimum time interval of the instrument, if any occurs. Therefore, the timestamps can be used to determine the time between the scattering events und thus the measured value of t_{ave} per bin including the detection efficiency. The outcome depends on the PM mass concentration and is valid as long as the concentration remained constant in average. As soon as the average time between particles is known, the ratio $(t_{ave}/T)^{½}$ can be calculated and a more realistic value for the uncertainty per bin can be determined.

In the above road traffic example, the average mass in the 10µm bin was 6.6µg/m^3 and PM10 was 19µg/m^3. With 35% contribution to the PM mass in the 10µm bin, there is a good reason for trying to measure the 10µm bin accurately. From theory, we get a value of 3.97s for t_{ave}, the above measurement however reveals a value of 36s for t_{ave}. This discrepancy is clearly attributed to the counting efficiency that is only 10% (one physical scattering pulse is assigned to 10 counts). Whereas the theoretical calculations yield best possible values for t_{ave} assuming 100% efficiency, the realistic efficiency is worse with the consequence that the measurement time has to be increased accordingly. This reality case tells us that a measurement time of 100*36s=1h would be required to measure the 10µm bin with a 1σ uncertainty of 10%. In case the time resolution is chosen smaller, small mass concentration changes can't be distinguished anymore from statistical uncertainty.

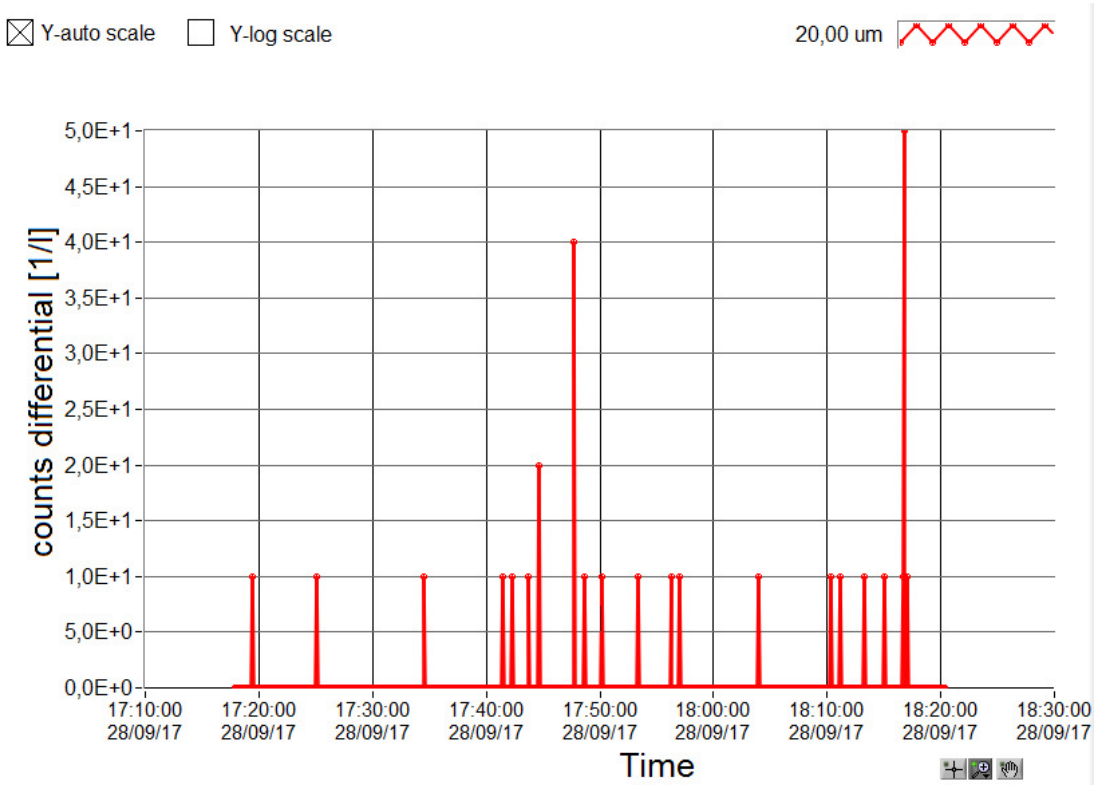

Fig. 5b: Display of the counts in the 20µm size bin versus time (Grimm 1.108 software)

To visualize the extraction of the mean time between particles in case of the Alphasense OPC-N2 low-cost sensor an experiment was run for measuring PM10 in a residential home. The sensor was put in a quiet cellar room and was run for almost 5 days. Fig. 6a shows the PM10 result over time with a resolution of 6s, whereas fig. 7 shows the counts of the 8-10µm bin taken from the logged histogram data.

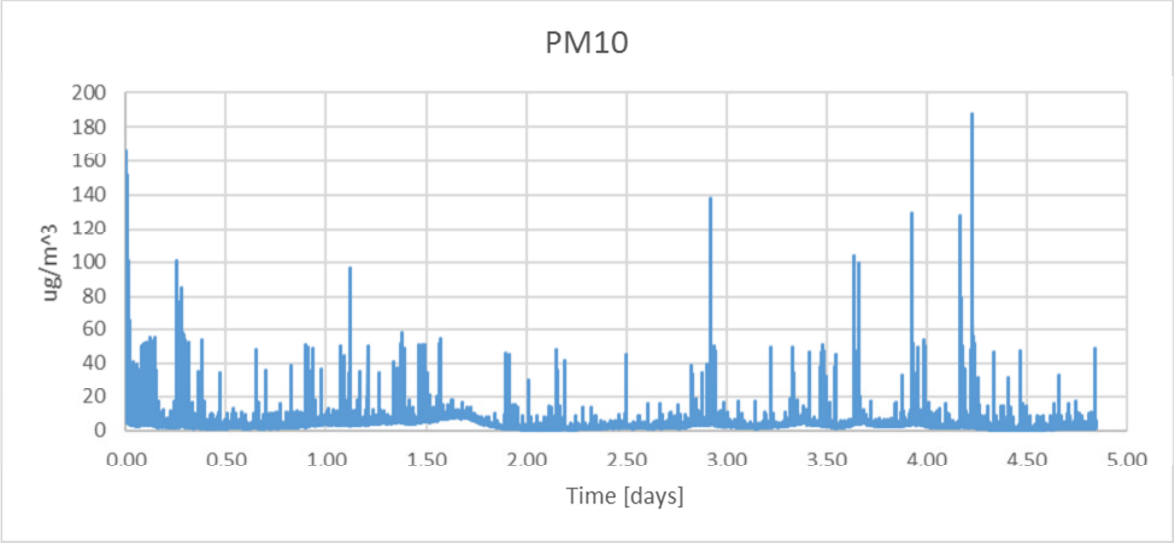

Fig. 6a: Measurement with the Alphasense OPC-N2 in the cellar of a residential house

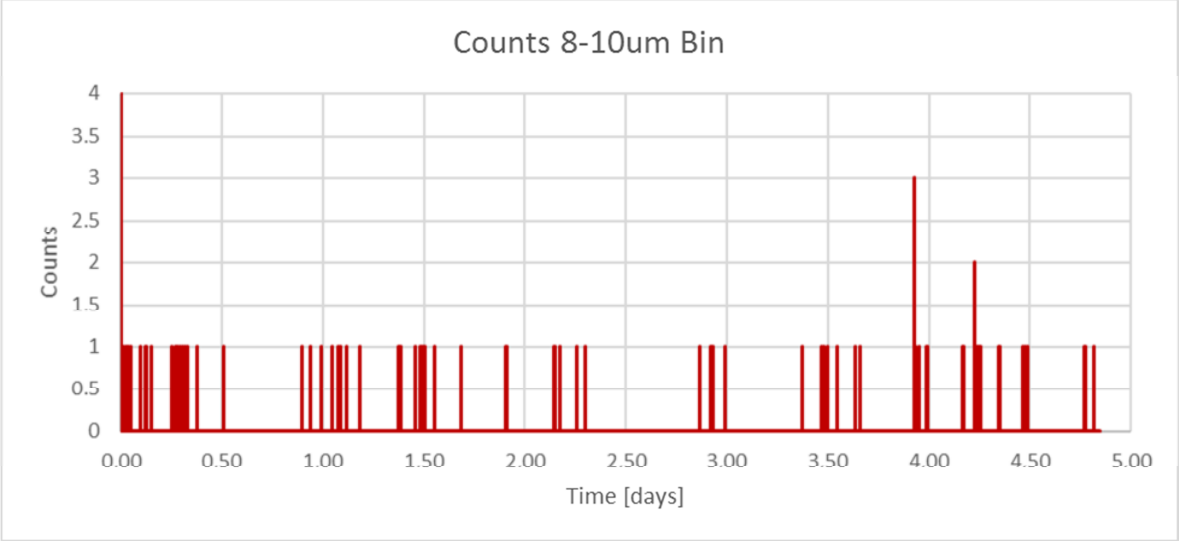

Fig. 6b: Counts in the 8-10µm bin of the OPC-N2 for the above measurement

The counts graph shows clearly that the dominant amount of laser scattering pulses in a measurement interval of the sensor occurred as single pulses and the times between occurrence are hours. Therefore, just from looking at this graph it becomes pretty obvious, that an accurate measurement requires a measurement interval of several days, otherwise statistical fluctuations may be larger than fluctuations of the mass concentration. Assuming that the mass concentration didn't vary too much, we can extract the average mean time between the detection of particles in the 8-10µm bin by the sensor. From the logfile we can determine an average PM10 value of 3.7µg/m^3, a mass concentration of 0.14 µg/m^3 and a mean time between particle arrival in the 10µm bin of t_{ave} = 38min. To achieve a 1σ uncertainty of 10% in the measurement, this means that a measurement

time T of 100*t_{ave} = 2.64 days is required. It also tells us, that a measurement result taken from a 5 days' average is accurate enough from the perspective of statistical fluctuations.

Conclusion

The above discussion shows that the statistical measurement uncertainties obtained from laser scattering PM-measurement instruments and laser scattering PM-sensors are similar to those of instruments and sensors counting particles in nuclear physics. The statistics of randomly arriving particles is governed by the Poisson theory. For the sample volume flows used in common laser scattering PM measuring devices, the particle count concentrations are small, particularly for large particles and small PM mass concentrations. As a result, the statistical fluctuation of measurement results can be high. Since each size bin contributes with its size specific uncertainty, the calculation of a characteristic value such as PM10 sums up all uncertainties. The key value important for determining the measurement uncertainty is the average lapse of time between particles as they randomly arrive in the measurement volume. In the above discussion, it is shown that measurement uncertainty of PM mass can be expressed simply by the squared ratio of the time between particles and the measurement time weighted by the respective mass concentration in a specific size bin. For determining the uncertainty of a PM10 measurement these size specific uncertainties can be summed up in a root mean square sense to estimate the PM10 uncertainty.

Comparing low-cost sensors such as the Alphasense OPC-N2 to professional equipment such as the Grimm 1.108 portable aerosol spectrometer, it becomes obvious that the required measurement times significantly increase when a similar accuracy is acquired. Particularly for mobile measurement this is an important aspect that needs to be considered, since long measurement times will limit spatial resolution when a certain speed is reached.

Literature

/1/ V. Wishnevsky, R.J. Schwankner und l. Gundelach; Düngemittel. Zur natürlichen Radioaktivität von Mineraldüngern. Praxis der Naturwissenschaften. Chemie, 38 (1989) 2, S. 33-35
https://www.fb06.fh-muenchen.de/fb/index.php/de/download.html?f_id=7656

/2/ S Pommé et al.; Uncertainty of nuclear counting; Metrologia 52 S3; 2015

/3/ Portable Laser Aerosolspectrometer and Dust Monitor Model 1.108/1.109; Grimm Aerosol Technik GmbH; Version V2-4 (24-10-14)

/4/ Laser PM2.5Sensor specification Productmodel SDS011 V1.3; Nova Fitness Co.,Ltd, China, 2015-10-9

/5/ OPC-N2 Particle Monitor, Technical specification; Alphasense Ltd, Sensor Technology, UK; May 2017

/6/ Timothy I. O'Hern and Daniel J. Rader; Practical application of in situ aerosol measurement; Engineering Sciences Center Sandia National Laboratories; Albuquerque, New Mexico 87185

/7/ Peter Siegel, Sephir Eskandari; Statistics of nuclear decay, Chapter 2 in Radiation Biology Notes
https://www.cpp.edu/~pbsiegel/bio431/texnotes/chapter2.pdf

/8/ Kumiko Fukutsu et al.; A Statistical Study on the Design of Particle Count Measurements; J. AerosolRes., Jpn-, 14 (1), 55-62 (1999)

/9/ Keith E. Holbert; Radiation counting statistics; School of Electrical, Computer and Energy Engineering, Arizona State University
http://holbert.faculty.asu.edu/eee460/RadiationCountingStatistics.pdf

/10/ J. Raasch, H. Umhauer; Grundsätzliche Überlegungen zur Messung der Verteilungen von Partikelgröße und Partikelgeschwindigkeit disperser Phasen in Strömungen;
Chem.-Ing.-Tech. 49(1977) Nr. 12, S.931-941